2009 American Control Conference
Hyatt Regency Riverfront, St. Louis, MO, USA
June 10-12, 2009



# Variance amplification in channel flows of strongly elastic polymer solutions

Mihailo R. Jovanović and Satish Kumar

***Abstract*— This paper identifies a new mechanism for amplification of stochastic disturbances in channel flows of strongly elastic polymer solutions. For streamwise constant flows with high elasticity numbers $\mu$ and non-vanishing Reynolds numbers $Re$, the $O(\mu Re^3)$ scaling of the variance amplification is established using singular perturbations techniques. This demonstrates that large variances can be maintained in stochastically driven flows occurring in weak inertial/strong elastic regimes. Mathematically, the amplification arises due to nonnormality of the governing equations and, physically, it is caused by the stretching of the polymer stresses by the background shear. The reported developments provide a possible route for a bypass transition to 'elastic turbulence' and suggest a novel method for efficient mixing in micro-fabricated straight channels.**

***Index Terms*— Elastic turbulence, microfluidic mixing, polymer additives, singular perturbations, variance amplification, viscoelastic fluids.**

## I. Introduction

Newtonian fluids, such as air and water at ordinary pressures and temperatures, transition to turbulence under the influence of inertia. On the other hand, recent experiments have shown that fluids containing long polymer chains may become turbulent even in low inertial regimes [1], [2]. Transition to turbulence in viscoelastic fluids is important from both fundamental and technological standpoints [3] as they are often encountered in industrial and biological flows. Improved understanding of transition mechanisms in viscoelastic fluids has broad applications in modern technology, including enhanced mixing in microfluidic devices through the addition of polymers [4].

Amplification of stochastic disturbances in channel flows of viscoelastic fluids has recently been investigated using linear systems theory [5]. Computations reported in Ref. [5] demonstrated that elasticity can produce considerable amplification of streamwise-constant disturbances even when inertial effects are relatively weak. This amplification is fundamentally nonmodal in nature: it cannot be described using the standard normal mode decomposition of classical hydrodynamic stability analysis. Rather, it arises due to nonnormal nature of the governing equations which introduces large receptivity to ambient disturbances.

For the streamwise-constant channel flows of viscoelastic fluids with spanwise wavenumber $k_z$, elasticity number $\mu$, and viscosity ratio $\beta$, an explicit scaling of the variance amplification (i.e., the $H_2$ norm) with the Reynolds number $Re$ was recently developed in Ref. [6],

$$E(k_z; Re, \beta, \mu) \;=\; f(k_z; \beta, \mu) Re \;+\; g(k_z; \beta, \mu) Re^3,$$

where $f$ and $g$ denote the $Re$-independent functions. This extends the Newtonian-fluid results [7], [8] to channel flows of viscoelastic fluids. In this paper, in order to gain insight into the conditions under which strong elasticity amplifies stochastic disturbances, we apply singular perturbation techniques to show that the variance amplification scales as

$$E(k_z; Re, \beta, \mu) \;\approx\; \hat{f}(k_z; \beta) Re \;+\; \hat{g}(k_z; \beta) \mu Re^3, \quad \mu \gg 1.$$

The product between $\mu$ and $Re^3$ in this expression indicates the subtle interplay between inertial and elastic forces in viscoelastic fluids with arbitrarily low (but non-vanishing) Reynolds numbers and high elasticity numbers.

## II. Governing equations

We consider incompressible channel flows of polymer solutions; see Fig. 1 for geometry. The non-dimensional momentum conservation, mass conservation, and constitutive equations for an Oldroyd-B fluid are given by [9], [10]

$$\begin{aligned} \mathbf{V}_{\tilde{t}} \;&=\; \tfrac{1}{Re}(\beta \nabla^2 \mathbf{V} + (1-\beta) \nabla \cdot \mathbf{T} - \nabla P) - \nabla_{\mathbf{V}} \mathbf{V} + \tilde{\mathbf{F}}, \\ 0 \;&=\; \nabla \cdot \mathbf{V}, \\ \mathbf{T}_{\tilde{t}} \;&=\; \tfrac{1}{We}(\nabla \mathbf{V} + (\nabla \mathbf{V})^T - \mathbf{T}) - \nabla_{\mathbf{V}} \mathbf{T} + \\ &\quad\; \mathbf{T} \cdot \nabla \mathbf{V} + (\mathbf{T} \cdot \nabla \mathbf{V})^T, \end{aligned} \tag{1}$$

where $\tilde{t}$ is time, $\mathbf{V}$ is the velocity vector, $P$ is the pressure, $\mathbf{T}$ is the polymeric contribution to the stress tensor, and $\tilde{\mathbf{F}}$ is the spatio-temporal body force. Subscript $\tilde{t}$ denotes a partial derivative with respect to time $\tilde{t}$, $\nabla$ is the gradient, and $\nabla_{\mathbf{V}} = \mathbf{V} \cdot \nabla$. These equations have been brought to a dimensionless form by scaling length with the channel half height $\delta$, velocity with the largest base velocity $U_o$, time with $\delta/U_o$, polymer stresses with $\eta_p U_o/\delta^2$, pressure with $(\eta_s + \eta_p) U_o/\delta$, and body force with $U_o^2/\delta$. Here, $\eta_p$ and $\eta_s$, respectively, denote the polymer and solvent viscosities, $\beta = \eta_s/(\eta_s + \eta_p)$ is the ratio of the solvent viscosity to the total viscosity, $Re = \rho U_o \delta/(\eta_s + \eta_p)$ is the Reynolds number, $We = \lambda U_o/\delta$ is the Weissenberg number, and $\lambda$ is the fluid relaxation time. Note that $\lambda$ describes how quickly polymer stresses decay to zero when fluid motion stops. Furthermore, the Weissenberg number can equivalently be written as $We = \mu Re$, where $\mu$ denotes the elasticity number; this quantity determines the ratio between the fluid relaxation time, $\lambda$, and the vorticity diffusion time, $\rho \delta^2/(\eta_s + \eta_p)$.

In the absence of polymers, i.e. for $\beta = 1$, fluid becomes

M. R. Jovanović is with the Department of Electrical and Computer Engineering, University of Minnesota, Minneapolis, MN 55455, USA (mihailo@umn.edu). Partially supported by the National Science Foundation under CAREER Award CMMI-06-44793.

S. Kumar is with the Department of Chemical Engineering and Materials Science, University of Minnesota, Minneapolis, MN 55455, USA (kumar@cems.umn.edu).

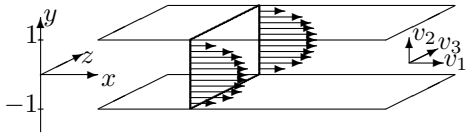


Fig. 1. Three dimensional channel flow.

Newtonian and system (1) simplifies to the incompressible Navier-Stokes equations. It is to be noted that the third equation in (1) describes history of deformation and it is obtained from a kinetic theory by representing each polymer molecule by an infinitely extensible Hookean spring connecting two spherical beads [9], [10]. This model is one of the simplest describing viscoelastic effects and is capable of predicting experimental observations in simple shear flows of elastic liquids with constant viscosity [3].

In flows with high elasticity numbers, $\epsilon = 1/\mu \ll 1$, it is more convenient to rescale time as $t = \tilde{t}/We$, which leads to the following set of equations:

$$\begin{aligned} \epsilon \mathbf{V}_t &= \beta\nabla^2\mathbf{V} + (1-\beta)\nabla\cdot\mathbf{T} - \nabla P - Re\,\nabla_{\mathbf{V}}\mathbf{V} + \sqrt{\epsilon Re}\,\mathbf{F}, \\ 0 &= \nabla\cdot\mathbf{V}, \\ \mathbf{T}_t &= \nabla\mathbf{V} + (\nabla\mathbf{V})^T - \mathbf{T} - (Re/\epsilon)\nabla_{\mathbf{V}}\mathbf{T} + (Re/\epsilon)(\mathbf{T}\cdot\nabla\mathbf{V} + (\mathbf{T}\cdot\nabla\mathbf{V})^T). \end{aligned} \tag{2}$$

Since we are interested in problems with stochastic spatio-temporal excitation, the body-forces in Eqs. (2) and (1) are related to each other by $\mathbf{F}(\mathbf{r},t) = \sqrt{We}\,\tilde{\mathbf{F}}(\mathbf{r}, t\ We)$, where $\mathbf{r}$ denotes the vector of spatial coordinates, $\mathbf{r} = [\ x\ \ y\ \ z\ ]^T$; this scaling is introduced to guarantee the same auto-correlation operators of $\mathbf{F}(\mathbf{r},t)$ and $\tilde{\mathbf{F}}(\mathbf{r},\tilde{t})$ [11].

Linearized dynamics are obtained by decomposing each field in (2) into the sum of the base flow and fluctuations (i.e., $\mathbf{V} = \overline{\mathbf{v}} + \mathbf{v}$, $\mathbf{T} = \overline{\boldsymbol{\tau}} + \boldsymbol{\tau}$, $P = \overline{p} + p$, $\mathbf{F} = 0 + \mathbf{d}$), and keeping terms only to first order in fluctuations:

$$\begin{aligned} \epsilon\dot{\mathbf{v}} &= -Re\,(\nabla_{\mathbf{v}}\overline{\mathbf{v}} + \nabla_{\overline{\mathbf{v}}}\mathbf{v}) - \nabla p + (1-\beta)\nabla\cdot\boldsymbol{\tau} + \beta\nabla^2\mathbf{v} + \sqrt{\epsilon Re}\,\mathbf{d}, \\ 0 &= \nabla\cdot\mathbf{v}, \\ \dot{\boldsymbol{\tau}} &= \nabla\mathbf{v} + (\nabla\mathbf{v})^T - \boldsymbol{\tau} + (Re/\epsilon)\big(-\nabla_{\mathbf{v}}\overline{\boldsymbol{\tau}} - \nabla_{\overline{\mathbf{v}}}\boldsymbol{\tau} + \boldsymbol{\tau}\cdot\nabla\overline{\mathbf{v}} + \overline{\boldsymbol{\tau}}\cdot\nabla\mathbf{v} + (\overline{\boldsymbol{\tau}}\cdot\nabla\mathbf{v})^T + (\boldsymbol{\tau}\cdot\nabla\overline{\mathbf{v}})^T\big). \end{aligned}$$

Here, a dot represents a partial derivative with respect to time $t$, $\mathbf{v} = [\ v_1\ \ v_2\ \ v_3\ ]^T$, where $v_1$, $v_2$, and $v_3$ are the velocity fluctuations in the streamwise ($x$), wall-normal ($y$), and spanwise ($z$) directions, respectively. In channel flows, the base velocity and polymer stress are given by

$$\overline{\mathbf{v}} = \begin{bmatrix} U(y) \\ 0 \\ 0 \end{bmatrix}, \quad \overline{\boldsymbol{\tau}} = \begin{bmatrix} 2We\,(U'(y))^2 & U'(y) & 0 \\ U'(y) & 0 & 0 \\ 0 & 0 & 0 \end{bmatrix},$$

with $U(y) = \{y,$ Couette flow; $1-y^2,$ Poiseuille flow$\}$, and $U'(y) = \mathrm{d}U(y)/\mathrm{d}y$.

The linearized momentum equation is driven by the body force fluctuation vector $\mathbf{d} = [\ d_1\ \ d_2\ \ d_3\ ]^T$, which is considered to be purely harmonic in the horizontal directions, and stochastic in the wall-normal direction and in time. This spatio-temporal body forcing will in turn yield velocity and polymer stress fluctuations of the same nature. Our objective is to study the steady-state variance of $\mathbf{v}$ by assuming that $\mathbf{d}$ is temporally stationary white Gaussian process with zero mean and unit variance.

We study the linearized model for streamwise-constant three-dimensional fluctuations, which means that the dynamics evolve in the $(y,z)$-plane, but flow fluctuations in three spatial directions are considered. This so-called two-dimensional three-component (2D/3C) model [12] is analyzed since the largest velocity variance in stochastically driven channel flows of viscoelastic fluids is maintained by streamwise-constant fluctuations [5].

### A. The streamwise-constant evolution model

The state-space representation of the linearized system is obtained by a standard conversion to the wall-normal velocity/vorticity $(v_2, \omega_2)$ formulation. The procedure described in Ref. [5] in combination with the Fourier transform in $z$-direction converts the governing equations with streamwise-constant fluctuations ($\partial_x(\cdot) \equiv 0$) to:

$$\begin{aligned} \epsilon\dot{\phi}_1 &= \beta S_{11}\phi_1 + (1-\beta)S_{12}\boldsymbol{\phi}_2 + \sqrt{\epsilon Re}\,(F_2 d_2 + F_3 d_3), \\ \dot{\boldsymbol{\phi}}_2 &= -\boldsymbol{\phi}_2 + S_{21}\phi_1, \\ \epsilon\dot{\phi}_3 &= \beta S_{33}\phi_3 + Re S_{31}\phi_1 + (1-\beta)S_{34}\boldsymbol{\phi}_4 + \sqrt{\epsilon Re}\,F_1 d_1, \\ \dot{\boldsymbol{\phi}}_4 &= -\boldsymbol{\phi}_4 + \tfrac{Re}{\epsilon}(S_{41}\phi_1 + S_{42}\boldsymbol{\phi}_2) + S_{43}\,\phi_3, \\ \dot{\phi}_5 &= -\phi_5 - \left(\tfrac{Re}{\epsilon}\right)^2 S_{51}\phi_1 + \tfrac{Re}{\epsilon}(S_{53}\,\phi_3 + S_{54}\,\boldsymbol{\phi}_4), \\ \begin{bmatrix} v_1 \\ v_2 \\ v_3 \end{bmatrix} &= \begin{bmatrix} 0 & G_1 \\ G_2 & 0 \\ G_3 & 0 \end{bmatrix} \begin{bmatrix} \phi_1 \\ \boldsymbol{\phi}_3 \end{bmatrix}, \end{aligned} \tag{3}$$

where $\phi_1 = v_2$, $\boldsymbol{\phi}_2 = [\tau_{22}\ \tau_{23}\ \tau_{33}]^T$, $\phi_3 = \omega_2$, $\boldsymbol{\phi}_4 = [\tau_{12}\ \tau_{13}]^T$, $\phi_5 = \tau_{11}$. The operators $F_j$ and $G_j$ are given by

$$F_1 = \mathrm{i}k_z,\ F_2 = -k_z^2\Delta^{-1},\ F_3 = -\mathrm{i}k_z\Delta^{-1}\partial_y,$$
$$G_1 = -(\mathrm{i}/k_z),\ G_2 = I,\ G_3 = (\mathrm{i}/k_z)\partial_y,$$

and they, respectively, describe the way the forcing enters into the state-space model, and the way the velocity fluctuations depend on the wall-normal velocity and vorticity. Here, $\mathrm{i} = \sqrt{-1}$, $k_z$ is the spanwise wavenumber, $I$ is the identity operator, $\Delta = \partial_{yy} - k_z^2$ is a Laplacian with homogeneous Dirichlet boundary conditions, and $\Delta^{-1}$ is the inverse of the Laplacian. Furthermore, the $S$-operators are given by:

$$\begin{aligned} &S_{11} = \Delta^{-1}\Delta^2, \quad S_{33} = \Delta, \quad S_{31} = -\mathrm{i}k_z U'(y), \\ &S_{12} = \Delta^{-1}\begin{bmatrix} -k_z^2\partial_y & -\mathrm{i}k_z\left(\partial_{yy} + k_z^2\right) & k_z^2\partial_y \end{bmatrix}, \\ &S_{34} = \begin{bmatrix} \mathrm{i}k_z\partial_y & -k_z^2 \end{bmatrix}, \quad S_{43} = -(1/k_z^2)S_{34}^T, \\ &S_{21} = \begin{bmatrix} 2\partial_y & (\mathrm{i}/k_z)\left(\partial_{yy} + k_z^2\right) & -2\partial_y \end{bmatrix}^T, \\ &S_{41} = \begin{bmatrix} U'(y)\partial_y - U''(y) \\ (\mathrm{i}/k_z)U'(y)\partial_{yy} \end{bmatrix}, \\ &S_{42} = \begin{bmatrix} U'(y) & 0 & 0 \\ 0 & U'(y) & 0 \end{bmatrix}, \ S_{51} = 4U'(y)U''(y), \\ &S_{53} = -(2\mathrm{i}/k_z)U'(y)\partial_y, \quad S_{54} = \begin{bmatrix} 2U'(y) & 0 \end{bmatrix}, \end{aligned}$$

where $\Delta^2 = \partial_{yyyy} - 2k_z^2\partial_{yy} + k_z^4$ with homogeneous Cauchy (both Dirichlet and Neumann) boundary conditions. Note that (3) represents a system of PDEs in wall-normal direction and in time parameterized by $k_z$, $Re$, $\beta$, and $\epsilon$.

## III. Frequency response representation

Application of the temporal Fourier transform on (3) allows for elimination of the polymer stresses from the equations, which results in an equivalent block diagram representation of the linearized 2D/3C system. All signals in Fig. 2 are functions of the wall-normal coordinate $y$, the spanwise wave-number $k_z$, and the temporal frequency $\omega$, e.g. $v_2 = v_2(y, k_z, \omega)$, with the following boundary conditions on $v_2$ and $\omega_2$, $\{v_2(\pm 1, k_z, \omega) = \partial_y v(\pm 1, k_z, \omega) = \omega_2(\pm 1, k_z, \omega) = 0\}$. The capital letters in Fig. 2 denote the Reynolds-number-independent operators. These operators act in the wall-normal direction and some of them are parameterized by $k_z$ ($F_j$ and $G_j$, $j = 1, 2, 3$), while the others depend on $k_z$, $\omega$, $\beta$, and $\epsilon$ ($J_1$, $J_2$, and $C_p$). The operator $C_p$ captures the coupling from $v_2$ to $\omega_2$, and it is defined as

$$C_p \;=\; C_{p1} \;+\; \frac{1}{\epsilon(1 \,+\, \mathrm{i}\omega)^2} C_{p2},$$

where $C_{p1} = -\mathrm{i}k_z U'(y)$ denotes the vortex tilting term, and

$$C_{p2} \;=\; \mathrm{i}k_z(1-\beta)\tilde{C}_{p2},\;\; \tilde{C}_{p2} \;=\; U'(y)\Delta + 2U''(y)\partial_y,$$

denotes the term arising due to the work done by the polymer stresses on the flow. Finally, $J_1$ and $J_2$ govern the internal dynamics of the wall-normal vorticity and velocity fluctuations, respectively. These two operators are given by

$$J_j = (1+\mathrm{i}\omega)K_j,\;\; K_j = \left(\epsilon(\mathrm{i}\omega)^2 I - (\beta T_j - \epsilon I)\mathrm{i}\omega - T_j\right)^{-1},$$

where $T_1 = \Delta$ and $T_2 = \Delta^{-1}\Delta^2$, respectively, represent the Squire and Orr-Sommerfeld operators in the 2D/3C model of Newtonian fluids with $Re = 1$ [8].

In the frequency domain, the velocity and forcing components are related by $v_i = H_{ij} d_j$, where $H_{ij}$ denotes the $ij$th component of the frequency response operator $H$, $\mathbf{v} = H\mathbf{d}$. From Fig. 2, it is clear that the $H_{ij}$ are determined by

$$\begin{aligned}
H_{11}(k_z, \omega; Re, \beta, \epsilon) \;&=\; \sqrt{Re}\; \bar{H}_{11}(k_z, \omega; \beta, \epsilon),\\
H_{1j}(k_z, \omega; Re, \beta, \epsilon) \;&=\; \sqrt{Re^3}\; \bar{H}_{1j}(k_z, \omega; \beta, \epsilon),\;\; j = 2, 3,\\
H_{ij}(k_z, \omega; Re, \beta, \epsilon) \;&=\; \sqrt{Re}\; \bar{H}_{ij}(k_z, \omega; \beta, \epsilon),\;\; i, j = 2, 3,\\
H_{i1}(k_z, \omega; Re, \beta, \epsilon) \;&=\; 0,\;\; i = 2, 3,
\end{aligned}$$

where the $\bar{H}_{ij}$ represent the $Re$-independent operators,

$$\begin{aligned}
\bar{H}_{11} \;&=\; \sqrt{\epsilon}\, G_1 J_1 F_1,\\
\bar{H}_{1j} \;&=\; \sqrt{\epsilon}\, G_1 J_1 C_p J_2 F_j,\;\; j = 2, 3,\\
\bar{H}_{ij} \;&=\; \sqrt{\epsilon}\, G_i J_2 F_j,\;\; i, j = 2, 3.
\end{aligned}$$

The variance maintained in $\mathbf{v}$ is quantified by the $H_2$ norm

$$E(k_z) \;=\; \frac{1}{2\pi}\int_{-\infty}^{\infty} \mathrm{tr}\left(H(k_z, \omega) H^*(k_z, \omega)\right)\, \mathrm{d}\omega,$$

where $H^*$ is the adjoint of operator $H$, and tr is the trace operator. (For notational brevity we have omitted the dependence on $Re$, $\beta$, and $\epsilon$ in the last expression). Using the properties of the trace operator we have $E(k_z) = \sum_{i,j=1}^{3} E_{ij}(k_z)$, where $E_{ij}$ is the variance maintained in $v_i$ by stochastically forcing the 2D/3C model with $d_j$. From the definition of operators $H_{ij}$, the following $Re$-scaling of $E$ is readily obtained

$$E(k_z; Re, \beta, \epsilon) \;=\; f(k_z; \beta, \epsilon) Re \;+\; g(k_z; \beta, \epsilon) Re^3, \quad \text{(E)}$$

where

$$f \;=\; f_{11} \;+\; f_{22} \;+\; f_{23} \;+\; f_{32} \;+\; f_{33},\;\; g \;=\; g_{12} \;+\; g_{13},$$

with

$$f_{ij}(k_z) \;=\; \frac{1}{2\pi}\int_{-\infty}^{\infty} \mathrm{tr}\left(\bar{H}_{ij}(k_z, \omega)\bar{H}_{ij}^*(k_z, \omega)\right)\, \mathrm{d}\omega,$$

and similarly for $g_{1j}$. The expression (E) for the steady-state variance of $\mathbf{v}$ is valid for all $Re$, $\beta$, and $\epsilon$. Our objective is to establish how the $Re$-independent functions $f$ and $g$ depend on $\epsilon$ in viscoelastic flows with $\epsilon = 1/\mu \ll 1$ in order to gain insight into the conditions under which strong elasticity amplifies stochastic disturbances.

### A. State-space realizations of $\bar{H}_{ij}$

The Reynolds-number-independent contributions to the steady-state variance can be determined by recasting each $\bar{H}_{ij}$ in the state-space form

$$\begin{aligned}
\dot{x}_{ij}(y, k_z, t) \;&=\; A_{ij}(k_z) x_{ij}(y, k_z, t) \;+\; B_j(k_z) d_j(y, k_z, t),\\
v_i(y, k_z, t) \;&=\; C_i(k_z) x_{ij}(y, k_z, t),
\end{aligned}$$

where $x_{ij}$ is a vector of state variables, and $(d_j, v_i)$ is the input-output pair for frequency response $\bar{H}_{ij}$. It is a standard fact [13] that the variance of $v_i$ sustained by $d_j$ is determined by $\mathrm{tr}\left(P_{ij} C_i^* C_i\right)$, where $P_{ij}$ denotes the steady-state auto-correlation operator of $x_{ij}$, which is found by solving the Lyapunov equation,

$$A_{ij} P_{ij} \;+\; P_{ij} A_{ij}^* \;=\; -B_j B_j^*.$$

The frequency responses $\bar{H}_{ij}$ with $\{i, j = 2, 3;\, i = j = 1\}$ admit the controller canonical form realization

$$\begin{aligned}
\begin{bmatrix} \dot{x}_{ij} \\ \epsilon \dot{z}_{ij} \end{bmatrix} \;&=\; \begin{bmatrix} 0 & I \\ T_k & \beta T_k - \epsilon I \end{bmatrix} \begin{bmatrix} x_{ij} \\ z_{ij} \end{bmatrix} \;+\; \begin{bmatrix} 0 \\ F_j \end{bmatrix} d_j,\\
v_i \;&=\; \sqrt{\epsilon}\, \begin{bmatrix} G_i & G_i \end{bmatrix} \begin{bmatrix} x_{ij} \\ z_{ij} \end{bmatrix},
\end{aligned} \tag{4}$$

with $\{k = 1 \text{ for } i = 1;\; k = 2 \text{ for } i = 2, 3\}$, homogeneous Dirichlet boundary conditions on $x_{11}$ and $z_{11}$, and homogeneous Cauchy boundary conditions on $x_{ij}$ and $z_{ij}$ for $i, j = 2, 3$. On the other hand, from Fig. 3 and definition of operators $K_1$ and $K_2$, it follows that each $\bar{H}_{1j}$, $j = 2, 3$, can be represented by

$$\begin{aligned}
\epsilon\ddot{\psi} \;&=\; T_2\psi \;+\; (\beta T_2 - \epsilon I)\,\dot{\psi} \;+\; F_j d_j,\\
\epsilon\ddot{\phi} \;&=\; T_1\phi \;+\; (\beta T_1 - \epsilon I)\,\dot{\phi} \;+\; \varphi,\;\; v_1 \;=\; \sqrt{1/\epsilon}\, G_1\phi,\\
\varphi \;&=\; C_{p1}(\epsilon\ddot{\psi} + 2\epsilon\dot{\psi} + \epsilon\psi) \;+\; C_{p2}\psi,
\end{aligned}$$

with homogeneous Dirichlet boundary conditions on $\phi$, and homogeneous Cauchy boundary conditions on $\psi$. By selecting $x = [\;\psi\;\;\phi\;]^T$, $z = [\;\dot{\psi}\;\;\dot{\phi}\;]^T$, we obtain a singularly

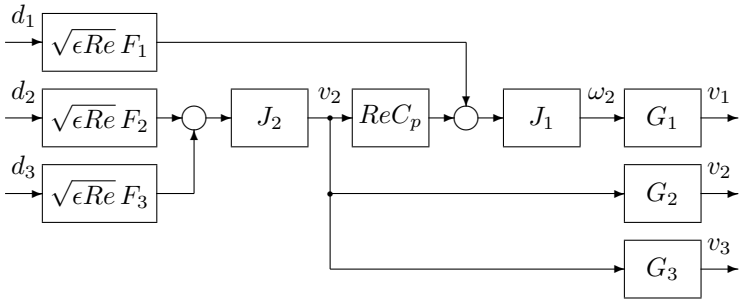


Fig. 2. Block diagram of the linearized 2D/3C model.

perturbed realization of $\bar{H}_{1j}$

$$\begin{aligned}\begin{bmatrix} \dot{x} \\ \epsilon\dot{z} \end{bmatrix} &= \begin{bmatrix} 0 & I \\ A_{21}(\epsilon) & A_{22}(\epsilon) \end{bmatrix}\begin{bmatrix} x \\ z \end{bmatrix} + \begin{bmatrix} 0 \\ B_2 \end{bmatrix} d_j, \\ v_1 &= \sqrt{1/\epsilon}\begin{bmatrix} C_1 & 0 \end{bmatrix}\begin{bmatrix} x \\ z \end{bmatrix},\end{aligned} \tag{5}$$

where all operators are partitioned conformably with the elements of $x$ and $z$,

$$A_{21} = \begin{bmatrix} T_2 & 0 \\ C_{p2} + C_{p1}(T_2 + \epsilon I) & T_1 \end{bmatrix},\ B_2 = \begin{bmatrix} F_j \\ C_{p1}F_j \end{bmatrix},$$
$$A_{22} = \begin{bmatrix} \beta T_2 - \epsilon I & 0 \\ C_{p1}(\beta T_2 + \epsilon I) & \beta T_1 - \epsilon I \end{bmatrix},\ C_1 = \begin{bmatrix} 0 & G_1 \end{bmatrix}.$$

Eqs. (4) and (5) are in the standard *singularly perturbed* form [11] as the time-derivative of the second part of the state is multiplied by a small positive parameter $\epsilon$ and the 22-block of operator $A$ at $\epsilon = 0$ is invertible.

## IV. Singular perturbation analysis of variance amplification

From Section III-A it follows that state-space realizations of operators $\bar{H}_{ij}$ assume the form

$$\begin{aligned}\begin{bmatrix} \dot{x} \\ \epsilon\dot{z} \end{bmatrix} &= \begin{bmatrix} 0 & I \\ A_{21}(\epsilon) & A_{22}(\epsilon) \end{bmatrix}\begin{bmatrix} x \\ z \end{bmatrix} + \begin{bmatrix} 0 \\ B_2 \end{bmatrix} d_j, \\ v_i &= r(\epsilon)\begin{bmatrix} C_1 & C_2 \end{bmatrix}\begin{bmatrix} x \\ z \end{bmatrix},\end{aligned} \tag{6}$$

with appropriate boundary conditions on $x$ and $z$, $r = \sqrt{\epsilon}$ for $\{i = j = 1;\ i, j = 2, 3\}$, and $r = 1/\sqrt{\epsilon}$ for $\{i = 1;\ j = 2, 3\}$. To simplify notation we have omitted $i$ and $j$ indices in Eq. (6); it is to be noted, however, that $x$, $z$, $r$, and $A$-operators depend on both $i$ and $j$, $B$-operators depend on $j$, and $C$-operators depend on $i$. The following coordinate transformation [11]

$$\begin{bmatrix} \xi \\ \eta \end{bmatrix} = \begin{bmatrix} I - \epsilon Q(\epsilon)L(\epsilon) & -\epsilon Q(\epsilon) \\ L(\epsilon) & I \end{bmatrix}\begin{bmatrix} x \\ z \end{bmatrix}, \tag{7}$$

can be utilized to fully separate the slow and fast dynamics of system (6). Namely, if $L(\epsilon)$ and $Q(\epsilon)$ satisfy

$$A_{21}(\epsilon) - A_{22}(\epsilon)L(\epsilon) - \epsilon L(\epsilon)L(\epsilon) = 0, \tag{L}$$
$$I - Q(\epsilon)\left(A_{22}(\epsilon) + \epsilon L(\epsilon)\right) - \epsilon L(\epsilon)Q(\epsilon) = 0, \tag{Q}$$

then the change of coordinates (7) brings system (6) to the following equivalent representation

$$\begin{aligned}\begin{bmatrix} \dot{\xi} \\ \dot{\eta} \end{bmatrix} &= \begin{bmatrix} A_s(\epsilon) & 0 \\ 0 & \frac{1}{\epsilon}A_f(\epsilon) \end{bmatrix}\begin{bmatrix} \xi \\ \eta \end{bmatrix} + \begin{bmatrix} B_s(\epsilon) \\ \frac{1}{\epsilon}B_f(\epsilon) \end{bmatrix} d_j, \\ v_i &= r(\epsilon)\begin{bmatrix} C_s(\epsilon) & C_f(\epsilon) \end{bmatrix}\begin{bmatrix} \xi \\ \eta \end{bmatrix},\end{aligned}$$

with

$$\begin{aligned} A_s &= -L(\epsilon), & A_f &= A_{22}(\epsilon) + \epsilon L(\epsilon), \\ B_s &= -Q(\epsilon)B_2, & B_f &= B_2, \\ C_s &= C_1 - C_2L(\epsilon), & C_f &= C_2 + \epsilon(C_1 - C_2L(\epsilon))Q(\epsilon). \end{aligned}$$

It is now easy to show that the steady-state auto-correlation operator of $\begin{bmatrix} \xi^T & \eta^T \end{bmatrix}^T$ takes the form

$$\bar{P}(\epsilon) = \begin{bmatrix} X(\epsilon) & Y^*(\epsilon) \\ Y(\epsilon) & (1/\epsilon)Z(\epsilon) \end{bmatrix},$$

where components of $\bar{P}$ are to be determined from the following system of equations

$$\begin{aligned} A_s(\epsilon)X(\epsilon) + X(\epsilon)A_s^*(\epsilon) &= -B_s(\epsilon)B_s^*(\epsilon), \\ A_f(\epsilon)Y(\epsilon) + \epsilon Y(\epsilon)A_s^*(\epsilon) &= -B_f(\epsilon)B_s^*(\epsilon), \\ A_f(\epsilon)Z(\epsilon) + Z(\epsilon)A_f^*(\epsilon) &= -B_f(\epsilon)B_f^*(\epsilon). \end{aligned} \tag{9}$$

This implies that the $H_2$ norm of operator $\bar{H}_{ij}$ is given by

$$\begin{aligned}\|\bar{H}_{ij}\|_2^2 &= r^2(\epsilon)\,\mathrm{tr}\big(X(\epsilon)C_s^*(\epsilon)C_s(\epsilon) + \tfrac{1}{\epsilon}Z(\epsilon)C_f^*(\epsilon)C_f(\epsilon)\big) \\ &+ r^2(\epsilon)\,\mathrm{tr}\big(Y(\epsilon)C_s^*(\epsilon)C_f(\epsilon) + Y^*(\epsilon)C_f^*(\epsilon)C_s(\epsilon)\big).\end{aligned} \tag{10}$$

Now, using the fact that $A_{21}(\epsilon)$ and $A_{22}(\epsilon)$ in Eqs. (4) and (5) are given by $\{A_{21}(\epsilon) = A_{21,0} + \epsilon A_{21,1};\ A_{22}(\epsilon) = A_{22,0} + \epsilon A_{22,1}\}$, we represent $L$ and $Q$ as $L(\epsilon) = \sum_{n=0}^{\infty}\epsilon^n L_n$, $Q(\epsilon) = \sum_{n=0}^{\infty}\epsilon^n Q_n$ and employ (regular) perturbation analysis to render (L) and (Q) into the following set of conveniently coupled equations:

$$\epsilon^0:\ \begin{cases} L_0 = A_{22,0}^{-1}A_{21,0}, \\ Q_0 = A_{22,0}^{-1}, \end{cases}$$
$$\epsilon^1:\ \begin{cases} L_1 = A_{22,0}^{-1}\left(A_{21,1} - A_{22,1}L_0 - L_0L_0\right), \\ Q_1 = -\left(L_0Q_0 + Q_0\left(A_{22,1} + L_0\right)\right)A_{22,0}^{-1}, \end{cases}$$
$$\vdots$$

Thus, $\Pi(\epsilon) = \sum_{n=0}^{\infty}\epsilon^n\Pi_n$ where $\Pi$ stands for $A_s$, $A_f$, $B_s$, $C_s$, or $C_f$, and similar procedure can be used to simplify (9) and determine coefficients in the power series expansions of

operators $X$, $Y$, and $Z$

$$\epsilon^0: \begin{cases} A_{s,0}X_0 + X_0A_{s,0}^* &= -B_{s,0}B_{s,0}^*, \\ A_{f,0}Y_0 &= -B_fB_{s,0}^*, \\ A_{f,0}Z_0 + Z_0A_{f,0}^* &= -B_fB_f^*, \end{cases}$$

$$\epsilon^1: \begin{cases} A_{s,0}X_1 + X_1A_{s,0}^* &= -\left(A_{s,1}X_0 + X_0A_{s,1}^*\right) \\ & \quad -\left(B_{s,0}B_{s,1}^* + B_{s,1}B_{s,0}^*\right), \\ A_{f,0}Y_1 + B_fB_{s,1}^* &= -\left(A_{f,1}Y_0 + Y_0A_{s,0}^*\right), \\ A_{f,0}Z_1 + Z_1A_{f,0}^* &= -\left(A_{f,1}Z_0 + Z_0A_{f,1}^*\right), \\ & \vdots \end{cases}$$

*Remark 1:* Even though the above developments are motivated by finite-dimensional methods for singularly perturbed systems [11], it can be shown that these methods extend to infinite dimensional problems considered in this paper. In particular, for the streamwise constant model existence of $L(\epsilon)$ and $Q(\epsilon)$ satisfying (L) and (Q) can be established. These technical results are not presented here due to page constraints and they will be reported elsewhere.

### A. Scaling of function $f$ in equation (E) with $\epsilon$

We now consider the $\epsilon$-scaling of function $f$ in the expression for the steady-state velocity variance. As shown in Section III, $f(k_z;\beta,\epsilon) = \sum_{i,j} f_{ij}(k_z;\beta,\epsilon)$, $\{i=j=1; i,j=2,3\}$, where $f_{ij}$ denotes the square of the $H_2$ norm of system (4). A direct comparison of Eqs. (4) and (6) yields $r(\epsilon) = \sqrt{\epsilon}$, $A_{21} = T_k$, $A_{22} = \beta T_k - \epsilon I$, $B_2 = F_j$, $C_1 = C_2 = G_i$, which in combination with Eq. (10) can be used to obtain

$$f(k_z;\beta,\epsilon) \;=\; \hat{f}_0(k_z;\beta) \;+\; \sum_{n=1}^{\infty} \epsilon^n \hat{f}_n(k_z;\beta).$$

Here, $\hat{f}_n$ are functions independent of $\epsilon$. Thus, in flows with $\epsilon \ll 1$, the terms contributing to the $Re$-scaling of the steady-state variance in Eq. (E) approximately become $\epsilon$-independent, i.e.

$$f(k_z;\beta,\epsilon) \;=\; \hat{f}_0(k_z;\beta) \;+\; O(\epsilon),$$

where $\hat{f}_0(k_z;\beta)$ is determined by the terms of the form $\mathrm{tr}\,(Z_0C_{f,0}^*C_{f,0})$, with $A_{f,0}Z_0 + Z_0A_{f,0}^* = -B_fB_f^*$.

### B. Scaling of function $g$ in equation (E) with $\epsilon$

Next, we examine the $\epsilon$-dependence of terms responsible for the $Re^3$-scaling of the steady-state variance. As shown in Section III, $g(k_z;\beta,\epsilon) = \sum_{j=2}^{3} g_{1j}(k_z;\beta,\epsilon)$, where $g_{1j}$ denotes the square of the $H_2$ norm of system (5). By comparing Eqs. (5) and (6) we see that $r(\epsilon) = 1/\sqrt{\epsilon}$ and $C_2 \equiv 0$. The latter observation implies that $C_s = C_1$ is $\epsilon$-independent and that $C_f(\epsilon) = \epsilon C_1 Q(\epsilon)$, which together with Eq. (10) can be used to obtain

$$g_{1j} \;=\; (1/\epsilon)\,\mathrm{tr}\,(X_0C_1^*C_1) \;+\; O(1).$$

In fact, it can be shown that

$$g(k_z;\beta,\epsilon) \;=\; \frac{1}{\epsilon}\sum_{n=0}^{\infty} \epsilon^n \hat{g}_n(k_z;\beta), \quad \epsilon \ll 1,$$

where $\hat{g}_0(k_z;\beta)$ is determined by $\mathrm{tr}\,(X_0C_1^*C_1)$.

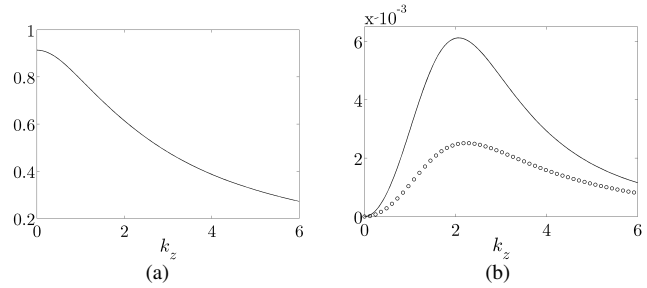


Fig. 4. Plots of $\tilde{f}_0(k_z)$ (a) and $\tilde{g}_0(k_z)$ (b); $\tilde{g}_0(k_z)$ in both Couette (solid curve) and Poiseuille (circles) flows is shown.

## V. Main result: implications and discussions

The developments of Section IV are summarized in the following Theorem.

*Theorem 1:* In streamwise-constant channel flows of Oldroyd-B fluids with $\mu \gg 1$, the steady-state variance of $\mathbf{v}$ is given by

$$E(k_z;Re,\beta,\mu) \;\approx\; Re\hat{f}_0(k_z;\beta) \;+\; \mu Re^3\hat{g}_0(k_z;\beta),$$

where $\hat{f}_0$ and $\hat{g}_0$ are functions independent of $Re$ and $\mu$.

Thus, in elasticity-dominated flows, the terms responsible for the $Re$- and $Re^3$-scaling of the steady-state variance are, respectively, $\mu$-independent and linearly dependent on $\mu$. It is readily shown that

$$\hat{f}_0(k_z;\beta) \;=\; \tilde{f}_0(k_z)/\beta,$$

where the base-flow-independent function $\tilde{f}_0(k_z)$ is given by

$$\tilde{f}_0(k_z) \;=\; -0.5\left(\mathrm{tr}\,(T_1^{-1}) + \mathrm{tr}\,(T_2^{-1})\right).$$

Furthermore,

$$\hat{g}_0(k_z;\beta) \;=\; \tilde{g}_0(k_z)(1-\beta)^2/\beta,$$

with

$$\tilde{g}_0(k_z) \;=\; (k_z^2/4)\,\mathrm{tr}\left(T_1^{-1}\tilde{C}_{p2}T_2^{-2}\tilde{C}_{p2}^*T_1^{-1}\right).$$

Thus, for $\mu \gg 1$,

$$E(k_z;Re,\beta,\mu) \;\approx\; \frac{Re}{\beta}\left(\tilde{f}_0(k_z) \;+\; \mu Re^2(1-\beta)^2\tilde{g}_0(k_z)\right),$$

which shows that the variance depends affinely on $\mu$ and increases monotonically with a decrease in the ratio of the solvent viscosity to the total viscosity. This expression should be compared to the expression for the variance amplification in Newtonian fluids [7],

$$E_N(k_z;Re) \;=\; Re f_N(k_z) \;+\; Re^3 g_N(k_z).$$

At low $Re$-values the $k_z$-dependence of $E_N$ is governed by $f_N(k_z)$, and at high $Re$-values $E_N(k_z) \approx Re^3 g_N(k_z)$ [7]. In fluids containing long polymer chains, however, even in low inertial regimes the spectrum of $E$ can be dominated by the $Re^3$-term owing to the elastic amplification of disturbances. Our results thus uncover the subtle interplay between inertial and elastic forces in Oldroyd-B fluids with low Reynolds/high elasticity numbers.

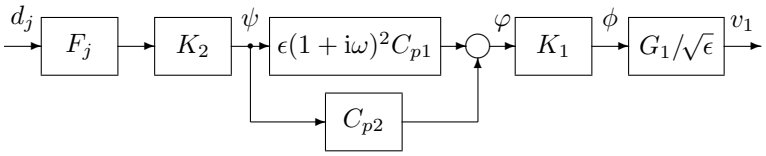


Fig. 3. Block diagram of $\bar{H}_{1j}(k_z, \omega; \beta, \epsilon)$, $j = 2, 3$.

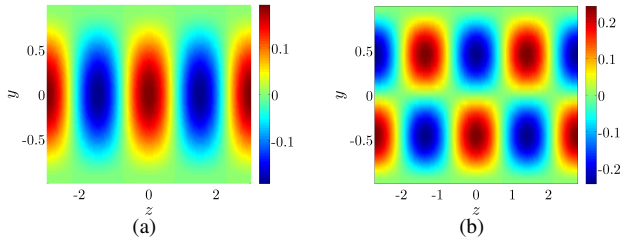


Fig. 5. Streamwise velocity fluctuations $v_1(z, y)$ containing most variance in Couette (a) and Poiseuille (b) flows.

The analytical expressions for $\mathrm{tr}\,(T_j^{-1})$, $j = 1, 2$, were derived in [7]; these can be used to obtain a formula for $\tilde{f}_0(k_z) = f_N(k_z)$, which is illustrated in Fig. 4(a). In Couette flow, the expression for $\tilde{g}_0(k_z)$ simplifies to $-(k_z^2/4)\,\mathrm{tr}\,(T_2^{-2}T_1^{-1})$, and an explicit $k_z$-dependence of $\tilde{g}_0$ can be derived after some manipulation. From Fig. 4(b) we observe the non-monotonic character of $\tilde{g}_0(k_z)$, with peak values at $k_z \approx 2.07$ (in Couette flow) and $k_z \approx 2.24$ (in Poiseuille flow). Streamwise velocity flow structures that contain the most variance in respective flows with these two spanwise wavenumbers are shown in Fig. 5. The most amplified sets of fluctuations are given by high (hot colors) and low (cold colors) speed streaks. In Couette flow the streaks occupy the entire channel width, and in Poiseuille flow they are antisymmetric with respect to the channel's centerline. These flow structures have striking resemblance to the initial conditions responsible for the largest transient growth in Newtonian fluids [14]. Despite similarities, the fluctuations shown in Fig. 5 and in Ref. [14] arise due to fundamentally different physical mechanisms: in high $Re$-flows of Newtonian fluids, the vortex tilting is the main driving force for amplification; in high $\mu$/low $Re$-flows of viscoelastic fluids, it is the polymer stretching mechanism. Namely, from the expression for $\tilde{g}_0(k_z)$ it follows that the coupling operator $\tilde{C}_{p2}$ plays the crucial role in variance amplification. If this term was zero, the dynamics of weakly inertial/strongly elastic flows would be dominated by viscous dissipation. A careful examination of the governing equations shows that $\tilde{C}_{p2}$ arises due to the stretching of the polymer stress fluctuations by the background shear.

## VI. Concluding Remarks

For low Reynolds numbers, behavior of Newtonian fluids is dominated by viscous dissipation. As $Re$ increases, the influence of inertia becomes more important and at large enough $Re$'s these fluids transition to turbulence. Fluids containing long polymer chains, however, may become turbulent even in low inertial regimes [1], [2]. This phenomenon is referred to as 'elastic turbulence' and it may find use in promoting mixing in microfluidic devices where inertial effects are weak due to the small geometries [4]. This paper reveals the intricate interplay between inertial and elastic forces in viscoelastic fluids with arbitrarily low (but non-zero) Reynolds numbers and high elasticity numbers. It is established that, in this regime, the dynamics is no longer dominated by viscous dissipation but rather by the polymer stretching mechanism, which introduces large variance amplification of streamwise-constant perturbations. This demonstrates the importance of alternating regions of high and low streamwise velocity (i.e., streamwise streaks) in strongly elastic shear flows of non-Newtonian fluids.

Our success with uncovering a here-to-fore unknown explicit analytical expression for variance amplification using the singular perturbation techniques, points to the scaling and modeling steps as prerequisites for their application. Physical systems seldom appear in a form ready-made for singular perturbation analysis; scaling and modeling steps presented in this paper may be helpful in attempts to devise such steps for a broader class of physical problems.

## Acknowledgements

The first author would like to thank Professors D. D. Joseph and P. V. Kokotović for stimulating discussions.

## References

[1] R. G. Larson, "Turbulence without inertia," *Nature*, vol. 405, pp. 27–28, 2000.
[2] A. Groisman and V. Steinberg, "Elastic turbulence in a polymer solution flow," *Nature*, vol. 405, pp. 53–55, 2000.
[3] R. G. Larson, "Instabilities in viscoelastic flows," *Rheol. Acta*, vol. 31, pp. 213–263, 1992.
[4] A. Groisman and V. Steinberg, "Efficient mixing at low Reynolds numbers using polymer additives," *Nature*, vol. 410, pp. 905–908, 2001.
[5] N. Hoda, M. R. Jovanović, and S. Kumar, "Energy amplification in channel flows of viscoelastic fluids," *J. Fluid. Mech.*, vol. 601, pp. 407–424, 2008.
[6] ——, "Frequency responses of streamwise-constant perturbations in channel flows of Oldroyd-B fluids," *J. Fluid. Mech.*, vol. 625, pp. 411–434, 2009.
[7] B. Bamieh and M. Dahleh, "Energy amplification in channel flows with stochastic excitations," *Phys. Fluids*, vol. 13, pp. 3258–3269, 2001.
[8] M. R. Jovanović and B. Bamieh, "Componentwise energy amplification in channel flows," *J. Fluid Mech.*, vol. 534, pp. 145–183, 2005.
[9] R. B. Bird, C. F. Curtiss, R. C. Armstrong, and O. Hassager, *Dynamics of Polymeric Liquids*. Wiley, 1987, vol. 2.
[10] R. G. Larson, *The Structure and Rheology of Complex Fluids*. Oxford University Press, 1999.
[11] P. Kokotović, H. K. Khalil, and J. O'Reilly, *Singular perturbation methods in control: analysis and design*. SIAM, 1999.
[12] W. C. Reynolds and S. C. Kassinos, "One-point modeling of rapidly deformed homogeneous turbulence," *Proc. R. Soc. Lond. A*, vol. 451, no. 1941, pp. 87–104, 1995.
[13] K. Zhou, J. C. Doyle, and K. Glover, *Robust and optimal control*. Prentice Hall, 1996.
[14] K. M. Butler and B. F. Farrell, "Three-dimensional optimal perturbations in viscous shear flow," *Phys. Fluids A*, vol. 4, pp. 1637–1650, 1992.